Model-Independent Observation of Exotic Contributions to B0 →j /ψK+π- Decays

LHCb Collaboration

DOI:
10.1103/PhysRevLett.122.152002

Document Version
Publisher's PDF, also known as Version of record

Citation for published version (Harvard):
LHCb Collaboration 2019, 'Model-Independent Observation of Exotic Contributions to $B^0 \to j/\psi K^+\pi^-$ Decays', *Physical Review Letters*, vol. 122, no. 15, 152002. https://doi.org/10.1103/PhysRevLett.122.152002

Model-Independent Observation of Exotic Contributions to $B^0 \to J/\psi K^+\pi^-$ Decays

R. Aaij *et al.*[*]
(LHCb Collaboration)

(Received 17 January 2019; published 17 April 2019)

An angular analysis of $B^0 \to J/\psi K^+\pi^-$ decays is performed, using proton-proton collision data corresponding to an integrated luminosity of 3 fb^{-1} collected with the LHCb detector. The $m(K^+\pi^-)$ spectrum is divided into fine bins. In each $m(K^+\pi^-)$ bin, the hypothesis that the three-dimensional angular distribution can be described by structures induced only by K^* resonances is examined, making minimal assumptions about the $K^+\pi^-$ system. The data reject the K^*-only hypothesis with a large significance, implying the observation of exotic contributions in a model-independent fashion. Inspection of the $m(J/\psi\pi^-)$ vs $m(K^+\pi^-)$ plane suggests structures near $m(J/\psi\pi^-) = 4200$ and 4600 MeV.

DOI: 10.1103/PhysRevLett.122.152002

In the standard model, the quark model allows for hadrons comprising any number of valence quarks, as long as they are color-singlet states. Yet, after decades of searches, the reason why the vast majority of hadrons are built out of only quark-antiquark (meson) or three-quark (baryon) combinations remains a mystery. The best known exception is the $Z(4430)^-$ resonance with spin-parity 1^- and width $\Gamma = 172 \pm 13$ MeV [1–3] which has minimal quark content $c\bar{c}\,\bar{u}\,\bar{d}$, and is therefore manifestly exotic, i.e., has components that are neither quark-antiquark or three-quark combinations. The only confirmed decay of the $Z(4430)^-$ state is via $Z(4430)^- \to \psi(2S)\pi^-$, as seen in $B^0 \to \psi(2S)K^+\pi^-$ decays [1,4]. The corresponding $Z(4430)^- \to J/\psi\pi^-$ decay rate is suppressed by at least a factor of 10 [5]. The authors of Ref. [6] surmise that in a dynamical diquark picture, this is because of a larger overlap of the $Z(4430)^-$ radial wave function with the excited state $\psi(2S)$ than with the ground state J/ψ. For the $B^0 \to J/\psi K^+\pi^-$ channel, the Belle collaboration [5] has reported the observation of a new exotic $Z(4200)^-$ resonance decaying to $J/\psi\pi^-$ that might correspond to the structure in $m(\psi(2S)\pi^-)$ seen in Ref. [1] at around the same mass.

A generic concern in searches for broad exotic states like the $Z(4430)^-$ resonance is disentangling contributions from nonexotic components. For $B^0 \to \psi^{(\prime)}K^+\pi^-$ decays [7], the latter comprise different K^*_J resonances with spin J, that decay to $K^+\pi^-$. Figure 1 shows the K^*_J spectrum, which has multiple, overlapping, and poorly measured states. The bulk of the measurements come from the LASS $K^+\pi^-$ scattering experiment [8]. In particular, the decay $B^0 \to J/\psi K^+\pi^-$ is known to be dominated by K^*_J resonances, with an exotic fit fraction of only 2.4% [5], compared to a 10.3% contribution from the $Z(4430)^-$ for $B^0 \to \psi(2S)K^+\pi^-$ [9]. This smaller exotic fit fraction for the J/ψ case makes it pertinent to study the evidence of exotic contributions in a manner independent of the dominant but poorly understood K^*_J spectrum.

The *BABAR* collaboration [11] has performed a model-independent analysis of $B^0 \to \psi^{(\prime)}K^+\pi^-$ decays making minimal assumptions about the K^*_J spectrum, using two-dimensional (2D) moments in the variables $m(K^+\pi^-)$ and the K^+ helicity angle, θ_V. The key feature of this approach

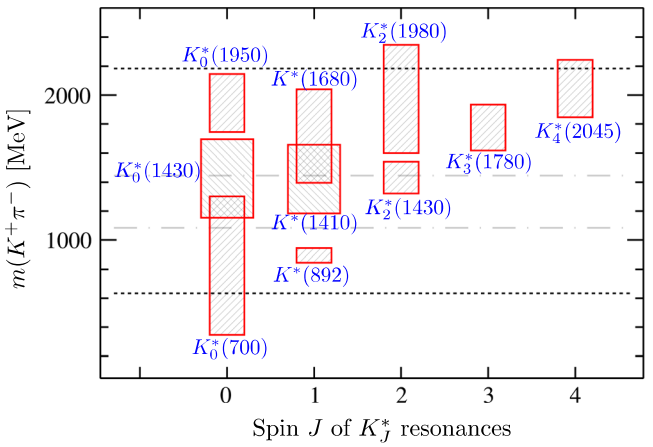

FIG. 1. Spectrum of K^*_J resonances from Ref. [10], with the vertical span of the boxes indicating $\pm\Gamma_0$, where Γ_0 is the width of each resonance. The horizontal dashed lines mark the $m(K^+\pi^-)$ physical region for $B^0 \to J/\psi K^+\pi^-$ decays, whereas the dot-dashed lines mark the specific region, $m(K^+\pi^-) \in [1085, 1445]$ MeV, employed for determining the significance of exotic contributions.

[*]Full author list given at the end of the article.

is that no information on the exact content of the K_J^* states, including their masses, widths, and $m(K^+\pi^-)$ -dependent line shapes, is required. An amplitude analysis would require the accurate description of the K_J^* line shapes which depend on the underlying production dynamics. The model-independent procedure bypasses these problems, requiring only knowledge of the highest spin, $J_{\max}$, among all the contributing K_J^* states, for a given $m(K^+\pi^-)$ bin. Within uncertainties, the $m(J/\psi\pi^-)$ spectrum in the *BABAR* data was found to be adequately described using just K_J^* states, without the need for exotic contributions.

In this Letter, a four-dimensional (4D) angular analysis of $B^0 \to J/\psi K^+\pi^-$ decays with $J/\psi \to \mu^+\mu^-$ is reported, employing the Run 1 LHCb dataset. The data sample corresponds to a signal yield approximately 40 and 20 times larger than those of the corresponding *BABAR* [11] and Belle [9] analyses, respectively. The larger sample size allows analysis of the differential rate as a function of the four variables, $m(K^+\pi^-)$, θ_V, θ_l, and χ, that fully describe the decay topology. The lepton helicity angle, θ_l, and the azimuthal angle, χ, between the $(\mu^+\mu^-)$ and $(K^+\pi^-)$ decay planes, were integrated over in the *BABAR* 2D analysis [11]. The present 4D analysis therefore benefits from a significantly better sensitivity to exotic components than the previous 2D analysis.

The LHCb detector is a single-arm forward spectrometer covering the pseudorapidity range $2 < \eta < 5$ and is described in detail in Ref. [12]. Samples of simulated events are used to obtain the detector efficiency and optimise the selection. The pp collisions are generated using PYTHIA [13] with a specific LHCb configuration [14]. Decays of hadronic particles are described by EVTGEN [15], in which final-state radiation is generated using PHOTOS [16]. Dedicated control samples are employed to calibrate the simulation for agreement with the data.

The selection procedure is the same as in Refs. [17,18] for the rare decay $B^0 \to \mu^+\mu^-K^+\pi^-$, with the additional requirement that the $m(\mu^+\mu^-)$ mass is constrained to the known J/ψ mass via a kinematic fit [19]. The data sample is divided into 35 fine bins in $m(K^+\pi^-)$ such that the $m(K^+\pi^-)$ dependence can be neglected inside a given bin, and each subsample is processed independently. The bin widths vary depending on the data sample size in a given $m(K^+\pi^-)$ region. Backgrounds from $B^+ \to J/\psi K^+$, $B_s^0 \to J/\psi K^+K^-$, and $\Lambda_b^0 \to J/\psi pK^-$ decays are reduced to a level below 1% of the signal yield at the selection stage using the excellent tracking and particle-identification capabilities of the LHCb detector, and are subsequently removed by a background subtraction procedure. The $B_{(s)}^0 \to J/\psi K^+\pi^-$ signal line shape in the $m(J/\psi K^+\pi^-)$ spectrum is described by a bifurcated Gaussian core and exponential tails on both sides. A sum of two such line shapes is used for the signal template for the mass fit, while the background line shape is a falling exponential. The exponential tails in the signal line shape are fixed from the simulation and all other parameters are allowed to vary in the fit, performed as a binned χ^2 minimization. An example mass fit result is given in the Supplemental Material [20]. The cumulative signal yield in the $m(K^+\pi^-) \in [745, 1545]$ MeV region is $554,500 \pm 800$.

The strategy in this analysis is to examine the hypothesis that nonexotic K_J^* contributions alone can explain all features of the data. Under the approximation that the muon mass can be neglected and within a narrow $m(K^+\pi^-)$ bin, the CP -averaged transition matrix element squared is [21,22]

$$|\mathcal{M}|^2 = \sum_{\eta} \Big| \sum_{\lambda,J} \sqrt{2J+1}\, \mathcal{H}_\lambda^{\eta,J} d^J_{\lambda,0}(\theta_V) d^1_{\lambda,\eta}(\theta_l) e^{i\lambda\chi} \Big|^2, \quad (1)$$

where $\mathcal{H}_\lambda^{\eta,J}$ are the K_J^* helicity amplitudes and $d^j_{m',m}$ are Wigner rotation matrix elements. The helicities of the outgoing lepton and K_J^* are $\eta = \pm 1$ and $\lambda \in \{0, \pm 1\}$, respectively. Parity conservation in the electromagnetic $J/\psi \to \mu^-\mu^+$ decay leads to the relation $\mathcal{H}_\lambda^{+,J} = \mathcal{H}_\lambda^{-,J} \equiv \mathcal{H}_\lambda^J$. The differential decay rate of $B^0 \to J/\psi(\to \mu^+\mu^-)K^+\pi^-$ with the $K^+\pi^-$ system including spin-J partial waves with $J \le J^k_{\max}$ can be written as

$$\left(\frac{d\Gamma^k}{d\Omega}\right)_{J^k_{\max}} \propto \sum_{i=1}^{n^k_{\max}} f_i(\Omega)\Gamma_i^k, \quad (2)$$

where the angular part in Eq. (1) has been expanded in an orthonormal basis of angular functions, $f_i(\Omega)$. Here, k enumerates the $m(K^+\pi^-)$ bin under consideration, and $\mathrm{d}\Omega = \mathrm{d}\cos\theta_\ell \mathrm{d}\cos\theta_V \mathrm{d}\chi$ is the angular phase space differential element. The angular basis functions, $f_i(\Omega)$, are constructed from spherical harmonics, $Y_l^m \equiv Y_l^m(\theta_l, \chi)$, and reduced spherical harmonics, $P_l^m \equiv \sqrt{2\pi} Y_l^m(\theta_V, 0)$, and are given in the Supplemental Material [20].

The Γ_i^k moments are observables that have an overall $m(K^+\pi^-)$ dependence, but within a narrow $m(K^+\pi^-)$ bin, this dependence can be neglected. The number of moments for the kth bin, $n^k_{\max}$, depends on the allowed spin of the highest partial wave, $J^k_{\max}$, and is given by Ref. [22]

$$n^k_{\max} = 28 + 12 \times (J^k_{\max} - 2), \quad \text{for } J^k_{\max} > 2. \quad (3)$$

Thus, for spin 3 onward, each additional higher spin component leads to 12 additional moments. In contrast to previous analyses, $\mathrm{d}\cos\theta_\ell \mathrm{d}\chi$ is not integrated over, which would have resulted in integrating over 10 out of these 12 moments, for each additional spin. Because of the orthonormality of the $f_i(\Omega)$ basis functions, the angular observables, Γ_i^k, can be determined from the data in an unbiased fashion using a simple counting measurement [21]. For the kth $m(K^+\pi^-)$ bin, the background-subtracted raw moments are estimated as

$$\Gamma^k_{i,\mathrm{raw}} = \sum_{p=1}^{n^k_{\mathrm{sig}}} f_i(\Omega_p) - x^k \sum_{p=1}^{n^k_{\mathrm{bkg}}} f_i(\Omega_p), \tag{4}$$

where Ω_p refers to the set of angles for a given event in this $m(K^+\pi^-)$ bin. The corresponding covariance matrix is

$$C^k_{ij,\mathrm{raw}} = \sum_{p=1}^{n^k_{\mathrm{sig}}} f_i(\Omega_p) f_j(\Omega_p) + (x^k)^2 \sum_{p=1}^{n^k_{\mathrm{bkg}}} f_i(\Omega_p) f_j(\Omega_p). \tag{5}$$

Here, n^k_{sig} and n^k_{bkg} correspond to the number of candidates in the signal and background regions, respectively. The signal region is defined within ± 15 MeV of the known B^0 mass, and the background region spans the range $m(J/\psi K^+\pi^-) \in [5450, 5560]$ MeV. The scale factor, x^k, is the ratio of the estimated number of background candidates in the signal region divided by the number of candidates in the background region and is used to normalize the background subtraction.

To unfold effects from the detector efficiency including event reconstruction and selection, an efficiency matrix, E^k_{ij}, is used. It is obtained from simulated signal events generated according to a phase space distribution, uniform in Ω, as

$$E^k_{ij} = \sum_{p=1}^{n^k_{\mathrm{sim}}} w^k_p f_i(\Omega_p) f_j(\Omega_p). \tag{6}$$

The w^k_p weight factors correct for differences between data and simulation, and the summation is over simulated and reconstructed events. They are derived using the $B^0 \to J/\psi K^*(892)^0$ control mode, as described in Refs. [17,18]. The efficiency-corrected moments and covariance matrices are estimated as

$$\Gamma^k_i = [(E^k)^{-1}]_{il} \Gamma^k_{l,\mathrm{raw}}, \tag{7}$$

$$C^k_{ij} = [(E^k)^{-1}]_{il} C^k_{lm,\mathrm{raw}} [(E^k)^{-1}]_{jm}. \tag{8}$$

The first moment, Γ^k_1, corresponds to the overall rate. The remaining moments and the covariance matrix are normalized to this overall rate as $\bar{\Gamma}^k_i \equiv \Gamma^k_i/\Gamma^k_1$ and

$$\bar{C}^k_{ij,\mathrm{stat}} = \left(\frac{C^k_{ij}}{(\Gamma^k_1)^2} + \frac{\Gamma^k_i \Gamma^k_j}{(\Gamma^k_1)^4} C^k_{11} - \frac{\Gamma^k_i C^k_{1j} + \Gamma^k_j C^k_{1i}}{\Gamma^k_1 (\Gamma^k_1)^2} \right), \tag{9}$$

for $i, j \in \{2, \ldots, n^k_{\mathrm{max}}\}$.

The normalization with respect to the total rate renders the analysis insensitive to any overall systematic effect not correlated with $\mathrm{d}\Omega$ in a given $m(K^+\pi^-)$ bin. The uncertainty from limited knowledge of the background is included in the second term in Eq. (5). The effect on the normalized moments, $\bar{\Gamma}^k_i$, due to the uncertainty in the x^k scale factors from the mass fit, is found to be negligible. The effect due to the limited simulation sample size compared to the data is small and accounted for using pseudoexperiments. The last source of systematic uncertainty is the effect of finite resolution in the reconstructed angles. The estimated biases in the measured $\bar{\Gamma}^k_i$ moments are added as additional uncertainties.

The dominant contributions to $B^0 \to J/\psi K^+\pi^-$ are from the $K^*(892)^0$ and $K^*_2(1430)^0$ states. To maximize the sensitivity to any exotic component, the dominant $K^*(892)^0$ region that serves as a background for any non-K^*_J component, the analysis is performed on the $m(K^+\pi^-) \in [1085, 1445]$ MeV region, as marked by the dot-dashed lines in Fig. 1. The value of J^k_{max} depends on $m(K^+\pi^-)$, with higher spin states suppressed at lower $m(K^+\pi^-)$ values, due to the orbital angular momentum barrier factor [23]. As seen from Fig. 1, only states with spin $J = \{0, 1\}$ contribute below $m(K^+\pi^-) \sim 1300$ MeV and spin $J = \{0, 1, 2\}$ below $m(K^+\pi^-) \sim 1600$ MeV. As a conservative choice, J^k_{max} is taken to be one unit larger than these expectations

$$J^k_{\mathrm{max}} = \begin{cases} 2 & \text{for } 1085 \le m(K^+\pi^-) < 1265 \text{ MeV}, \\ 3 & \text{for } 1265 \le m(K^+\pi^-) < 1445 \text{ MeV}. \end{cases} \tag{10}$$

Any exotic component in the $J/\psi\pi^-$ or $J/\psi K^+$ system will reflect onto the entire basis of K^*_J partial waves and give rise to nonzero contributions from $P_l(\cos\theta_V)$ components for l larger than those needed to account for K^*_J resonances. From the completeness of the $f_i(\Omega)$ basis, a model with large enough J^k_{max} also describes any exotic component in the data. For a given value of $m(K^+\pi^-)$, there is a one-to-one correspondence between $\cos\theta_V$ and the variables $m(J/\psi\pi^-)$ or $m(J/\psi K^+)$. Therefore, a complete basis of $P_l(\cos\theta_V)$ partial waves also describes any arbitrary shape in $m(J/\psi\pi^-)$ or $m(J/\psi K^+)$, for a given $m(K^+\pi^-)$ bin. The series is truncated at a value large enough to describe the relevant features of the distribution in data, but not so large that it follows bin-by-bin statistical fluctuations. A value of $J^k_{\mathrm{max}} = 15$ is found to be suitable.

For the kth $m(K^+\pi^-)$ bin, the probability density function (pdf) for the J^k_{max} model is

$$\mathcal{P}_{J^k_{\mathrm{max}}}(\Omega) = \frac{1}{\sqrt{8\pi}} \left(\frac{1}{\sqrt{8\pi}} + \sum_{i=2}^{n^k_{J_{\mathrm{max}}}} \bar{\Gamma}^k_i f_i(\Omega) \right). \tag{11}$$

Simulated events generated uniformly in Ω, after incorporating detector efficiency effects and weighting by the pdf in Eq. (11), are expected to match the background-subtracted data. The background subtraction is performed using the *sPlot* technique [24], where the weights are determined from fits to the invariant $m(J/\psi K^+\pi^-)$

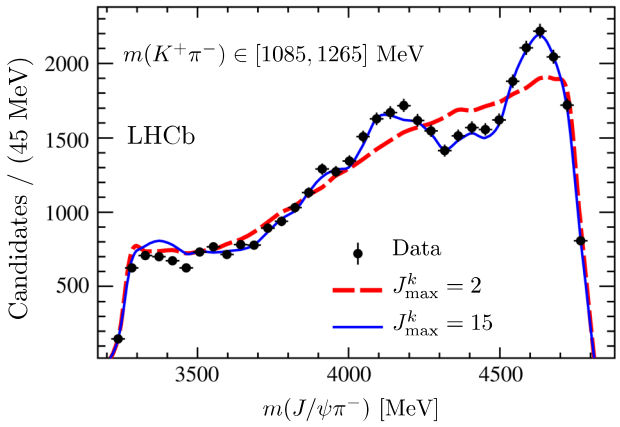

FIG. 2. Comparison of $m(J\psi\pi^-)$ in the $m(K^+\pi^-) \in [1085, 1265]$ MeV region between the background-subtracted data and simulated events weighted by moments models with $J^k_{\max} = 2$ and $J^k_{\max} = 15$.

distributions described previously. Figure 2 shows this comparison between the background-subtracted data and weighted simulated events in the $m(K^+\pi^-) \in [1085, 1265]$ MeV region. The $J^k_{\max} = 2$ model clearly misses the peaking structures in the data around $m(J/\psi\pi^-) = 4200$ and 4600 MeV. This inability of the $J^k_{\max} = 2$ model to describe the data, even though the first spin 2 state, $K^*_2(1430)^0$, lies beyond this mass region, strongly points toward the presence of exotic components. These could be four-quark bound states, meson molecules, or possibly dynamically generated features such as cusps.

To obtain a numerical estimate of the significance of exotic states, the likelihood ratio test is employed between the null hypothesis [K^*_J-only, from Eq. (10)] and the exotic hypothesis ($J^k_{\max} = 15$) pdfs, denoted as $\mathcal{P}^k_{K^*_J}$ and $\mathcal{P}^k_{\text{exotic}}$, respectively. The test statistic used in the likelihood ratio test is defined as

$$\begin{aligned}\Delta(-2\log\mathcal{L})|_k \equiv &-\sum_{p=1}^{n^k_{\text{sig}}} 2\log\frac{\mathcal{P}^k_{K^*_J}(\Omega_p)}{\mathcal{P}^k_{\text{exotic}}(\Omega_p)} \\ &+ x^k \sum_{p=1}^{n^k_{\text{bkg}}} 2\log\frac{\mathcal{P}^k_{K^*_J}(\Omega_p)}{\mathcal{P}^k_{\text{exotic}}(\Omega_p)} \\ &+ 2(n^k_{\text{sig}} - x^k n^k_{\text{bkg}})\log\frac{\int \mathcal{P}^k_{K^*_J}(\Omega)\epsilon(\Omega)\mathrm{d}\Omega}{\int \mathcal{P}^k_{\text{exotic}}(\Omega)\epsilon(\Omega)\mathrm{d}\Omega},\end{aligned} \tag{12}$$

for the kth $m(K^+\pi^-)$ bin, where $\epsilon(\Omega)$ denotes the three-dimensional angular detector efficiency in this bin, derived from the simulation weighted to match the data in the B^0 production kinematics. The last term in Eq. (12) ensures normalization of the relevant pdf and is calculated from simulated events that pass the reconstruction and selection criteria

$$E^k_i \equiv \sum_{p=1}^{n^k_{\text{sim}}} w^k_p f_i(\Omega_p), \tag{13}$$

$$\int \mathcal{P}_{J^k_{\max}}(\Omega)\epsilon(\Omega)\mathrm{d}\Omega \propto \sum_{i=1}^{n^k_{\max}} \Gamma^k_i E^k_i. \tag{14}$$

Results from individual $m(K^+\pi^-)$ bins are combined to give the final test statistic $\Delta(-2\log\mathcal{L}) = \sum_k \Delta(-2\log\mathcal{L})|_k$.

From Eq. (3) the number of degrees-of-freedom (ndf) increases by 12 for each additional spin-J wave in each $m(K^+\pi^-)$ bin. From Eq. (10), for the $J^k_{\max} = 2$ and 3 choices, $\Delta\text{ndf} = 12\times(15-2) = 156$ and $12\times(15-3) = 144$, respectively, between the exotic and K^*_J-only pdfs for each $m(K^+\pi^-)$ bin. Each additional degree-of-freedom between the exotic and K^*_J-only pdf adds approximately one unit to the computed $\Delta(-2\log\mathcal{L})$ in the data due to increased sensitivity to the statistical fluctuations, and $\Delta(-2\log\mathcal{L})$ is therefore not expected to be zero even if there is no exotic contribution in the data. The expected $\Delta(-2\log\mathcal{L})$ distribution in the absence of exotic activity is evaluated using a large number of pseudoexperiments. For each $m(K^+\pi^-)$ bin, 11 000 pseudoexperiments are generated according to the K^*_J-only model with the moments varied according to the covariance matrix. The number of signal and background events for each pseudoexperiment are taken to be those measured in the data. The detector efficiency obtained from simulation is parametrized in 4D. Each pseudoexperiment is analyzed in exactly the same way as the data, where an independent efficiency matrix is generated for each pseudoexperiment. This accounts for the limited sample size of the simulation for the efficiency unfolding. The pseudoexperiments therefore represent the data faithfully at every step of the processing.

Figure 3 shows the distribution of $\Delta(-2\log\mathcal{L})$ from the pseudoexperiments in the $m(K^+\pi^-) \in [1085, 1445]$ MeV

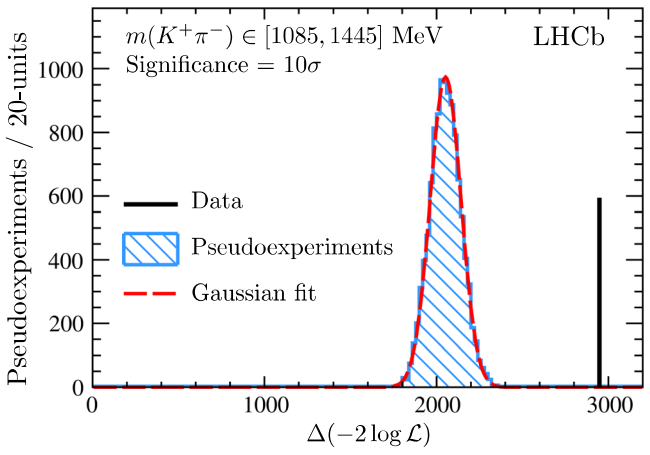

FIG. 3. Likelihood-ratio test for exotic significance. The data shows a 10σ deviation from the pseudoexperiments generated according to the null hypothesis (K^*_J-only contributions).

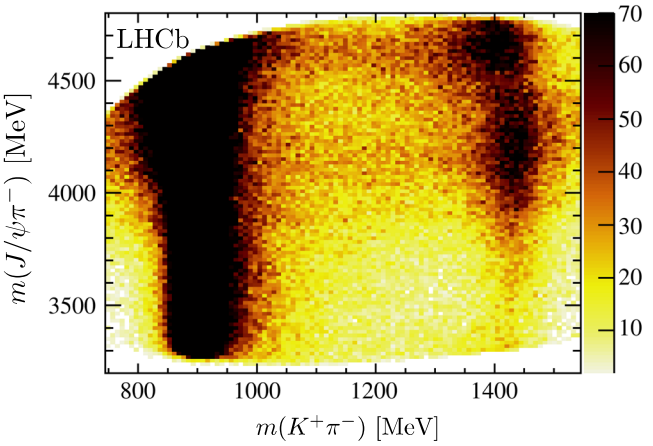

FIG. 4. Background-subtracted 2D distribution of $m(J/\psi\pi^-)$ vs $m(K^+\pi^-)$ in the region $m(K^+\pi^-) \in [745, 1545]$ MeV. The intensity (z-axis) scale has been highly truncated to limit the strong $K^*(892)^0$ contribution.

region comprising six $m(K^+\pi^-)$ bins each with the $J^k_{\max} = 2$ or 3 choice. A fit to a Gaussian profile gives $\Delta(-2\log\mathcal{L}) \approx 2051$ between the null and exotic hypothesis, even in the absence of any exotic contributions. This value is consistent with the naïve expectation $\Delta(\text{ndf}) = 1800$ from the counting discussed earlier. The value of $\Delta(-2\log\mathcal{L})$ for the data, as marked by the vertical line in Fig. 3, shows a deviation of more than 10σ from the null hypothesis, corresponding to the distribution of the pseudoexperiments. The uncertainty due to the quality of the Gaussian profile fit in Fig. 3 is found to be negligible. The choice of large $J^k_{\max}$ for $\mathcal{P}^k_{\text{exotic}}$, as well as the detector efficiency and calibration of the simulation, is systematically varied in pseudoexperiments, with significance for exotic components in excess of 6σ observed in each case.

In summary, employing the Run 1 LHCb dataset, non-K^*_J contributions in $B^0 \to J/\psi K^+\pi^-$ are observed with overwhelming significance. Compared to the previous *BABAR* analysis [11] of the same channel, the current study benefits from a 40-fold increase in signal yield and a full angular analysis of the decay topology. The method relies on a novel orthonormal angular moments expansion and, aside from a conservative limit on the highest allowed K^*_J spin for a given $m(K^+\pi^-)$ invariant mass, makes no other assumption about the $K^+\pi^-$ system. Figure 4 shows a scatter plot of $m(J/\psi\pi^-)$ against $m(K^+\pi^-)$ in the background-subtracted data. Although the model-independent analysis performed here does not identify the origin of the non-K^*_J contributions, structures are visible at $m(J/\psi\pi^-) \approx 4200$ MeV, close to the exotic state reported previously by Belle [5], and at $m(J/\psi\pi^-) \approx 4600$ MeV. To interpret these structures as exotic tetraquark resonances and measure their properties will require a future model-dependent amplitude analysis of the data.

We express our gratitude to our colleagues in the CERN accelerator departments for the excellent performance of the LHC. We thank the technical and administrative staff at the LHCb institutes. We acknowledge support from CERN and from the national agencies CAPES, CNPq, FAPERJ, and FINEP (Brazil); MOST and NSFC (China); CNRS/IN2P3 (France); BMBF, DFG, and MPG (Germany); INFN (Italy); NWO (Netherlands); MNiSW and NCN (Poland); MEN/IFA (Romania); MSHE (Russia); MinECo (Spain); SNSF and SER (Switzerland); NASU (Ukraine); STFC (United Kingdom); NSF (U.S.). We acknowledge the computing resources that are provided by CERN, IN2P3 (France), KIT and DESY (Germany), INFN (Italy), SURF (Netherlands), PIC (Spain), GridPP (United Kingdom), RRCKI and Yandex LLC (Russia), CSCS (Switzerland), IFIN-HH (Romania), CBPF (Brazil), PL-GRID (Poland), and OSC (U.S.). We are indebted to the communities behind the multiple open-source software packages on which we depend. Individual groups or members have received support from AvH Foundation (Germany); EPLANET, Marie Skłodowska-Curie Actions and ERC (European Union); ANR, Labex P2IO and OCEVU, and Région Auvergne-Rhône-Alpes (France); Key Research Program of Frontier Sciences of CAS, CAS PIFI, and the Thousand Talents Program (China); RFBR, RSF, and Yandex LLC (Russia); GVA, XuntaGal, and GENCAT (Spain); the Royal Society and the Leverhulme Trust (United Kingdom); Laboratory Directed Research and Development program of LANL (U.S.).

[1] R. Aaij *et al.* (LHCb Collaboration), Phys. Rev. Lett. **112**, 222002 (2014).
[2] S. K. Choi *et al.* (Belle Collaboration), Phys. Rev. Lett. **100**, 142001 (2008).
[3] Natural units with $\hbar = c = 1$ are used throughout the document.
[4] The inclusion of charge-conjugate decay modes is implied throughout.
[5] K. Chilikin *et al.* (Belle Collaboration), Phys. Rev. D **90**, 112009 (2014).
[6] S. J. Brodsky, D. S. Hwang, and R. F. Lebed, Phys. Rev. Lett. **113**, 112001 (2014).
[7] Here ψ denotes the ground state J/ψ, and ψ' denotes the excited state $\psi(2S)$.
[8] D. Aston *et al.* (LASS Collaboration), Nucl. Phys. **B296**, 493 (1988).
[9] K. Chilikin *et al.* (Belle Collaboration), Phys. Rev. D **88**, 074026 (2013).
[10] M. Tanabashi *et al.* (Particle Data Group), Phys. Rev. D **98**, 030001 (2018).
[11] B. Aubert *et al.* (*BABAR* Collaboration), Phys. Rev. D **79**, 112001 (2009).
[12] A. A. Alves, Jr. *et al.* (LHCb Collaboration), J. Instrum. **3**, S08005 (2008).

[13] T. Sjöstrand, S. Mrenna, and P. Skands, J. High Energy Phys. 05 (2006) 026; Comput. Phys. Commun. **178**, 852 (2008).
[14] I. Belyaev *et al.*, J. Phys. Conf. Ser. **331**, 032047 (2011).
[15] D. J. Lange, Nucl. Instrum. Methods Phys. Res., Sect. A **462**, 152 (2001).
[16] P. Golonka and Z. Was, Eur. Phys. J. C **45**, 97 (2006).
[17] R. Aaij *et al.* (LHCb Collaboration), J. High Energy Phys. 02 (2016) 104.
[18] R. Aaij *et al.* (LHCb Collaboration), J. High Energy Phys. 12 (2016) 065.
[19] W. D. Hulsbergen, Nucl. Instrum. Methods Phys. Res., Sect. A **552**, 566 (2005).
[20] See Supplemental Material at http://link.aps.org/supplemental/10.1103/PhysRevLett.122.152002 for definitions of the angles, an example mass fit, further comparisons between the data and moments models, and a list of the angular basis functions.
[21] B. Dey, Phys. Rev. D **92**, 033013 (2015).
[22] B. Dey, Phys. Rev. D **95**, 033004 (2017).
[23] F. von Hippel and C. Quigg, Phys. Rev. D **5**, 624 (1972).
[24] M. Pivk and F. R. Le Diberder, Nucl. Instrum. Methods Phys. Res., Sect. A **555**, 356 (2005).

R. Aaij,[29] C. Abellán Beteta,[46] B. Adeva,[43] M. Adinolfi,[50] C. A. Aidala,[77] Z. Ajaltouni,[7] S. Akar,[61] P. Albicocco,[20] J. Albrecht,[12] F. Alessio,[44] M. Alexander,[55] A. Alfonso Albero,[42] G. Alkhazov,[41] P. Alvarez Cartelle,[57] A. A. Alves Jr.,[43] S. Amato,[2] S. Amerio,[25] Y. Amhis,[9] L. An,[19] L. Anderlini,[19] G. Andreassi,[45] M. Andreotti,[18] J. E. Andrews,[62] F. Archilli,[29] J. Arnau Romeu,[8] A. Artamonov,[40] M. Artuso,[63] K. Arzymatov,[38] E. Aslanides,[8] M. Atzeni,[46] B. Audurier,[24] S. Bachmann,[14] J. J. Back,[52] S. Baker,[57] V. Balagura,[9,b] W. Baldini,[18] A. Baranov,[38] R. J. Barlow,[58] S. Barsuk,[9] W. Barter,[58] M. Bartolini,[21] F. Baryshnikov,[73] V. Batozskaya,[33] B. Batsukh,[63] A. Battig,[12] V. Battista,[45] A. Bay,[45] J. Beddow,[55] F. Bedeschi,[26] I. Bediaga,[1] A. Beiter,[63] L. J. Bel,[29] S. Belin,[24] N. Beliy,[4] V. Bellee,[45] N. Belloli,[22,c] K. Belous,[40] I. Belyaev,[35] G. Bencivenni,[20] E. Ben-Haim,[10] S. Benson,[29] S. Beranek,[11] A. Berezhnoy,[36] R. Bernet,[46] D. Berninghoff,[14] E. Bertholet,[10] A. Bertolin,[25] C. Betancourt,[46] F. Betti,[17,44] M. O. Bettler,[51] Ia. Bezshyiko,[46] S. Bhasin,[50] J. Bhom,[31] S. Bifani,[49] P. Billoir,[10] A. Birnkraut,[12] A. Bizzeti,[19,d] M. Bjørn,[59] M. P. Blago,[44] T. Blake,[52] F. Blanc,[45] S. Blusk,[63] D. Bobulska,[55] V. Bocci,[28] O. Boente Garcia,[43] T. Boettcher,[60] A. Bondar,[39,e] N. Bondar,[41] S. Borghi,[58,44] M. Borisyak,[38] M. Borsato,[43] F. Bossu,[9] M. Boubdir,[11] T. J. V. Bowcock,[56] C. Bozzi,[18,44] S. Braun,[14] M. Brodski,[44] J. Brodzicka,[31] A. Brossa Gonzalo,[52] D. Brundu,[24,44] E. Buchanan,[50] A. Buonaura,[46] C. Burr,[58] A. Bursche,[24] J. Buytaert,[44] W. Byczynski,[44] S. Cadeddu,[24] H. Cai,[67] R. Calabrese,[18,f] R. Calladine,[49] M. Calvi,[22,c] M. Calvo Gomez,[42,g] A. Camboni,[42,g] P. Campana,[20] D. H. Campora Perez,[44] L. Capriotti,[17,h] A. Carbone,[17,h] G. Carboni,[27] R. Cardinale,[21] A. Cardini,[24] P. Carniti,[22,c] K. Carvalho Akiba,[2] G. Casse,[56] L. Cassina,[22] M. Cattaneo,[44] G. Cavallero,[21] R. Cenci,[26,i] M. G. Chapman,[50] M. Charles,[10] Ph. Charpentier,[44] G. Chatzikonstantinidis,[49] M. Chefdeville,[6] V. Chekalina,[38] C. Chen,[3] S. Chen,[24] S.-G. Chitic,[44] V. Chobanova,[43] M. Chrzaszcz,[44] A. Chubykin,[41] P. Ciambrone,[20] X. Cid Vidal,[43] G. Ciezarek,[44] F. Cindolo,[17] P. E. L. Clarke,[54] M. Clemencic,[44] H. V. Cliff,[51] J. Closier,[44] V. Coco,[44] J. A. B. Coelho,[9] J. Cogan,[8] E. Cogneras,[7] L. Cojocariu,[34] P. Collins,[44] T. Colombo,[44] A. Comerma-Montells,[14] A. Contu,[24] G. Coombs,[44] S. Coquereau,[42] G. Corti,[44] M. Corvo,[18,f] C. M. Costa Sobral,[52] B. Couturier,[44] G. A. Cowan,[54] D. C. Craik,[60] A. Crocombe,[52] M. Cruz Torres,[1] R. Currie,[54] F. Da Cunha Marinho,[2] C. L. Da Silva,[78] E. Dall'Occo,[29] J. Dalseno,[43,j] C. D'Ambrosio,[44] A. Danilina,[35] P. d'Argent,[14] A. Davis,[3] O. De Aguiar Francisco,[44] K. De Bruyn,[44] S. De Capua,[58] M. De Cian,[45] J. M. De Miranda,[1] L. De Paula,[2] M. De Serio,[16,k] P. De Simone,[20] J. A. de Vries,[29] C. T. Dean,[55] D. Decamp,[6] L. Del Buono,[10] B. Delaney,[51] H.-P. Dembinski,[13] M. Demmer,[12] A. Dendek,[32] D. Derkach,[74] O. Deschamps,[7] F. Desse,[9] F. Dettori,[56] B. Dey,[68] A. Di Canto,[44] P. Di Nezza,[20] S. Didenko,[73] H. Dijkstra,[44] F. Dordei,[24] M. Dorigo,[44,l] A. C. dos Reis,[1] A. Dosil Suárez,[43] L. Douglas,[55] A. Dovbnya,[47] K. Dreimanis,[56] L. Dufour,[44] G. Dujany,[10] P. Durante,[44] J. M. Durham,[78] D. Dutta,[58] R. Dzhelyadin,[40] M. Dziewiecki,[14] A. Dziurda,[31] A. Dzyuba,[41] S. Easo,[53] U. Egede,[57] V. Egorychev,[35] S. Eidelman,[39,e] S. Eisenhardt,[54] U. Eitschberger,[12] R. Ekelhof,[12] L. Eklund,[55] S. Ely,[63] A. Ene,[34] S. Escher,[11] S. Esen,[29] T. Evans,[61] A. Falabella,[17] C. Färber,[44] N. Farley,[49] S. Farry,[56] D. Fazzini,[22,44,c] M. Féo,[44] P. Fernandez Declara,[44] A. Fernandez Prieto,[43] F. Ferrari,[17] L. Ferreira Lopes,[45] F. Ferreira Rodrigues,[2] M. Ferro-Luzzi,[44] S. Filippov,[37] R. A. Fini,[16] M. Fiorini,[18,f] M. Firlej,[32] C. Fitzpatrick,[45] T. Fiutowski,[32] F. Fleuret,[9,b] M. Fontana,[44] F. Fontanelli,[21,m] R. Forty,[44] V. Franco Lima,[56] M. Frank,[44] C. Frei,[44] J. Fu,[23,n] W. Funk,[44] E. Gabriel,[54] A. Gallas Torreira,[43] D. Galli,[17,h] S. Gallorini,[25] S. Gambetta,[54] Y. Gan,[3] M. Gandelman,[2] P. Gandini,[23] Y. Gao,[3] L. M. Garcia Martin,[76] J. García Pardiñas,[46] B. Garcia Plana,[43] J. Garra Tico,[51] L. Garrido,[42] D. Gascon,[42] C. Gaspar,[44] L. Gavardi,[12] G. Gazzoni,[7] D. Gerick,[14] E. Gersabeck,[58] M. Gersabeck,[58] T. Gershon,[52] D. Gerstel,[8] Ph. Ghez,[6] V. Gibson,[51] O. G. Girard,[45] P. Gironella Gironell,[42] L. Giubega,[34]

K. Gizdov,[54] V. V. Gligorov,[10] C. Göbel,[65] D. Golubkov,[35] A. Golutvin,[57,73] A. Gomes,[1,o] I. V. Gorelov,[36] C. Gotti,[22,c] E. Govorkova,[29] J. P. Grabowski,[14] R. Graciani Diaz,[42] L. A. Granado Cardoso,[44] E. Graugés,[42] E. Graverini,[46] G. Graziani,[19] A. Grecu,[34] R. Greim,[29] P. Griffith,[24] L. Grillo,[58] L. Gruber,[44] B. R. Gruberg Cazon,[59] O. Grünberg,[70] C. Gu,[3] E. Gushchin,[37] A. Guth,[11] Yu. Guz,[40,44] T. Gys,[44] T. Hadavizadeh,[59] C. Hadjivasiliou,[7] G. Haefeli,[45] C. Haen,[44] S. C. Haines,[51] B. Hamilton,[62] X. Han,[14] T. H. Hancock,[59] S. Hansmann-Menzemer,[14] N. Harnew,[59] T. Harrison,[56] C. Hasse,[44] M. Hatch,[44] J. He,[4] M. Hecker,[57] K. Heinicke,[12] A. Heister,[12] K. Hennessy,[56] L. Henry,[76] M. Heß,[70] J. Heuel,[11] A. Hicheur,[64] R. Hidalgo Charman,[58] D. Hill,[59] M. Hilton,[58] P. H. Hopchev,[45] J. Hu,[14] W. Hu,[68] W. Huang,[4] Z. C. Huard,[61] W. Hulsbergen,[29] T. Humair,[57] M. Hushchyn,[74] D. Hutchcroft,[56] D. Hynds,[29] P. Ibis,[12] M. Idzik,[32] P. Ilten,[49] A. Inglessi,[41] A. Inyakin,[40] K. Ivshin,[41] R. Jacobsson,[44] J. Jalocha,[59] E. Jans,[29] B. K. Jashal,[76] A. Jawahery,[62] F. Jiang,[3] M. John,[59] D. Johnson,[44] C. R. Jones,[51] C. Joram,[44] B. Jost,[44] N. Jurik,[59] S. Kandybei,[47] M. Karacson,[44] J. M. Kariuki,[50] S. Karodia,[55] N. Kazeev,[74] M. Kecke,[14] F. Keizer,[51] M. Kelsey,[63] M. Kenzie,[51] T. Ketel,[30] E. Khairullin,[38] B. Khanji,[44] C. Khurewathanakul,[45] K. E. Kim,[63] T. Kirn,[11] V. S. Kirsebom,[45] S. Klaver,[20] K. Klimaszewski,[33] T. Klimkovich,[13] S. Koliiev,[48] M. Kolpin,[14] R. Kopecna,[14] P. Koppenburg,[29] I. Kostiuk,[29] S. Kotriakhova,[41] M. Kozeiha,[7] L. Kravchuk,[37] M. Kreps,[52] F. Kress,[57] P. Krokovny,[39,e] W. Krupa,[32] W. Krzemien,[33] W. Kucewicz,[31,p] M. Kucharczyk,[31] V. Kudryavtsev,[39,e] A. K. Kuonen,[45] T. Kvaratskheliya,[35,44] D. Lacarrere,[44] G. Lafferty,[58] A. Lai,[24] D. Lancierini,[46] G. Lanfranchi,[20] C. Langenbruch,[11] T. Latham,[52] C. Lazzeroni,[49] R. Le Gac,[8] R. Lefèvre,[7] A. Leflat,[36] F. Lemaitre,[44] O. Leroy,[8] T. Lesiak,[31] B. Leverington,[14] P.-R. Li,[4,q] Y. Li,[5] Z. Li,[63] X. Liang,[63] T. Likhomanenko,[72] R. Lindner,[44] F. Lionetto,[46] V. Lisovskyi,[9] G. Liu,[66] X. Liu,[3] D. Loh,[52] A. Loi,[24] I. Longstaff,[55] J. H. Lopes,[2] G. H. Lovell,[51] D. Lucchesi,[25,r] M. Lucio Martinez,[43] A. Lupato,[25] E. Luppi,[18,f] O. Lupton,[44] A. Lusiani,[26] X. Lyu,[4] F. Machefert,[9] F. Maciuc,[34] V. Macko,[45] P. Mackowiak,[12] S. Maddrell-Mander,[50] O. Maev,[41,44] K. Maguire,[58] D. Maisuzenko,[41] M. W. Majewski,[32] S. Malde,[59] B. Malecki,[44] A. Malinin,[72] T. Maltsev,[39,e] G. Manca,[24,s] G. Mancinelli,[8] D. Marangotto,[23,n] J. Maratas,[7,t] J. F. Marchand,[6] U. Marconi,[17] C. Marin Benito,[9] M. Marinangeli,[45] P. Marino,[45] J. Marks,[14] P. J. Marshall,[56] G. Martellotti,[28] M. Martinelli,[44] D. Martinez Santos,[43] F. Martinez Vidal,[76] A. Massafferri,[1] M. Materok,[11] R. Matev,[44] A. Mathad,[52] Z. Mathe,[44] C. Matteuzzi,[22] A. Mauri,[46] E. Maurice,[9,b] B. Maurin,[45] M. McCann,[57,44] A. McNab,[58] R. McNulty,[15] J. V. Mead,[56] B. Meadows,[61] C. Meaux,[8] N. Meinert,[70] D. Melnychuk,[33] M. Merk,[29] A. Merli,[23,n] E. Michielin,[25] D. A. Milanes,[69] E. Millard,[52] M.-N. Minard,[6] L. Minzoni,[18,f] D. S. Mitzel,[14] A. Mödden,[12] A. Mogini,[10] R. D. Moise,[57] T. Mombächer,[12] I. A. Monroy,[69] S. Monteil,[7] M. Morandin,[25] G. Morello,[20] M. J. Morello,[26,u] O. Morgunova,[72] J. Moron,[32] A. B. Morris,[8] R. Mountain,[63] F. Muheim,[54] M. Mukherjee,[68] M. Mulder,[29] D. Müller,[44] J. Müller,[12] K. Müller,[46] V. Müller,[12] C. H. Murphy,[59] D. Murray,[58] P. Naik,[50] T. Nakada,[45] R. Nandakumar,[53] A. Nandi,[59] T. Nanut,[45] I. Nasteva,[2] M. Needham,[54] N. Neri,[23,n] S. Neubert,[14] N. Neufeld,[44] R. Newcombe,[57] T. D. Nguyen,[45] C. Nguyen-Mau,[45,v] S. Nieswand,[11] R. Niet,[12] N. Nikitin,[36] A. Nogay,[72] N. S. Nolte,[44] A. Oblakowska-Mucha,[32] V. Obraztsov,[40] S. Ogilvy,[55] D. P. O'Hanlon,[17] R. Oldeman,[24,s] C. J. G. Onderwater,[71] A. Ossowska,[31] J. M. Otalora Goicochea,[2] T. Ovsiannikova,[35] P. Owen,[46] A. Oyanguren,[76] P. R. Pais,[45] T. Pajero,[26,u] A. Palano,[16] M. Palutan,[20] G. Panshin,[75] A. Papanestis,[53] M. Pappagallo,[54] L. L. Pappalardo,[18,f] W. Parker,[62] C. Parkes,[58,44] G. Passaleva,[19,44] A. Pastore,[16] M. Patel,[57] C. Patrignani,[17,h] A. Pearce,[44] A. Pellegrino,[29] G. Penso,[28] M. Pepe Altarelli,[44] S. Perazzini,[44] D. Pereima,[35] P. Perret,[7] L. Pescatore,[45] K. Petridis,[50] A. Petrolini,[21,m] A. Petrov,[72] S. Petrucci,[54] M. Petruzzo,[23,n] B. Pietrzyk,[6] G. Pietrzyk,[45] M. Pikies,[31] M. Pili,[59] D. Pinci,[28] J. Pinzino,[44] F. Pisani,[44] A. Piucci,[14] V. Placinta,[34] S. Playfer,[54] J. Plews,[49] M. Plo Casasus,[43] F. Polci,[10] M. Poli Lener,[20] A. Poluektov,[52] N. Polukhina,[73,w] I. Polyakov,[63] E. Polycarpo,[2] G. J. Pomery,[50] S. Ponce,[44] A. Popov,[40] D. Popov,[49,13] S. Poslavskii,[40] E. Price,[50] J. Prisciandaro,[43] C. Prouve,[43] V. Pugatch,[48] A. Puig Navarro,[46] H. Pullen,[59] G. Punzi,[26,i] W. Qian,[4] J. Qin,[4] R. Quagliani,[10] B. Quintana,[7] N. V. Raab,[15] B. Rachwal,[32] J. H. Rademacker,[50] M. Rama,[26] M. Ramos Pernas,[43] M. S. Rangel,[2] F. Ratnikov,[38,74] G. Raven,[30] M. Ravonel Salzgeber,[44] M. Reboud,[6] F. Redi,[45] S. Reichert,[12] F. Reiss,[10] C. Remon Alepuz,[76] Z. Ren,[3] V. Renaudin,[59] S. Ricciardi,[53] S. Richards,[50] K. Rinnert,[56] P. Robbe,[9] A. Robert,[10] A. B. Rodrigues,[45] E. Rodrigues,[61] J. A. Rodriguez Lopez,[69] M. Roehrken,[44] S. Roiser,[44] A. Rollings,[59] V. Romanovskiy,[40] A. Romero Vidal,[43] M. Rotondo,[20] M. S. Rudolph,[63] T. Ruf,[44] J. Ruiz Vidal,[76] J. J. Saborido Silva,[43] N. Sagidova,[41] B. Saitta,[24,s] V. Salustino Guimaraes,[65] C. Sanchez Gras,[29] C. Sanchez Mayordomo,[76] B. Sanmartin Sedes,[43] R. Santacesaria,[28] C. Santamarina Rios,[43] M. Santimaria,[20,44] E. Santovetti,[27,x] G. Sarpis,[58] A. Sarti,[20,y] C. Satriano,[28,z] A. Satta,[27] M. Saur,[4] D. Savrina,[35,36] S. Schael,[11] M. Schellenberg,[12] M. Schiller,[55] H. Schindler,[44] M. Schmelling,[13] T. Schmelzer,[12] B. Schmidt,[44] O. Schneider,[45] A. Schopper,[44] H. F. Schreiner,[61] M. Schubiger,[45] S. Schulte,[45] M. H. Schune,[9]

R. Schwemmer,[44] B. Sciascia,[20] A. Sciubba,[28,y] A. Semennikov,[35] E. S. Sepulveda,[10] A. Sergi,[49] N. Serra,[46] J. Serrano,[8] L. Sestini,[25] A. Seuthe,[12] P. Seyfert,[44] M. Shapkin,[40] Y. Shcheglov,[41,a] T. Shears,[56] L. Shekhtman,[39,e] V. Shevchenko,[72] E. Shmanin,[73] B. G. Siddi,[18] R. Silva Coutinho,[46] L. Silva de Oliveira,[2] G. Simi,[25,r] S. Simone,[16,k] I. Skiba,[18] N. Skidmore,[14] T. Skwarnicki,[63] M. W. Slater,[49] J. G. Smeaton,[51] E. Smith,[11] I. T. Smith,[54] M. Smith,[57] M. Soares,[17] l. Soares Lavra,[1] M. D. Sokoloff,[61] F. J. P. Soler,[55] B. Souza De Paula,[2] B. Spaan,[12] E. Spadaro Norella,[23,n] P. Spradlin,[55] F. Stagni,[44] M. Stahl,[14] S. Stahl,[44] P. Stefko,[45] S. Stefkova,[57] O. Steinkamp,[46] S. Stemmle,[14] O. Stenyakin,[40] M. Stepanova,[41] H. Stevens,[12] A. Stocchi,[9] S. Stone,[63] B. Storaci,[46] S. Stracka,[26] M. E. Stramaglia,[45] M. Straticiuc,[34] U. Straumann,[46] S. Strokov,[75] J. Sun,[3] L. Sun,[67] Y. Sun,[62] K. Swientek,[32] A. Szabelski,[33] T. Szumlak,[32] M. Szymanski,[4] Z. Tang,[3] A. Tayduganov,[8] T. Tekampe,[12] G. Tellarini,[18] F. Teubert,[44] E. Thomas,[44] M. J. Tilley,[57] V. Tisserand,[7] S. T'Jampens,[6] M. Tobin,[32] S. Tolk,[44] L. Tomassetti,[18,f] D. Tonelli,[26] D. Y. Tou,[10] R. Tourinho Jadallah Aoude,[1] E. Tournefier,[6] M. Traill,[55] M. T. Tran,[45] A. Trisovic,[51] A. Tsaregorodtsev,[8] G. Tuci,[26,i] A. Tully,[51] N. Tuning,[29,44] A. Ukleja,[33] A. Usachov,[9] A. Ustyuzhanin,[38,74] U. Uwer,[14] A. Vagner,[75] V. Vagnoni,[17] A. Valassi,[44] S. Valat,[44] G. Valenti,[17] M. van Beuzekom,[29] E. van Herwijnen,[44] J. van Tilburg,[29] M. van Veghel,[29] A. Vasiliev,[40] R. Vazquez Gomez,[44] P. Vazquez Regueiro,[43] C. Vázquez Sierra,[29] S. Vecchi,[18] J. J. Velthuis,[50] M. Veltri,[19,aa] G. Veneziano,[59] A. Venkateswaran,[63] M. Vernet,[7] M. Veronesi,[29] M. Vesterinen,[52] J. V. Viana Barbosa,[44] D. Vieira,[4] M. Vieites Diaz,[43] H. Viemann,[70] X. Vilasis-Cardona,[42,g] A. Vitkovskiy,[29] M. Vitti,[51] V. Volkov,[36] A. Vollhardt,[46] D. Vom Bruch,[10] B. Voneki,[44] A. Vorobyev,[41] V. Vorobyev,[39,e] N. Voropaev,[41] R. Waldi,[70] J. Walsh,[26] J. Wang,[5] M. Wang,[3] Y. Wang,[68] Z. Wang,[46] D. R. Ward,[51] H. M. Wark,[56] N. K. Watson,[49] D. Websdale,[57] A. Weiden,[46] C. Weisser,[60] M. Whitehead,[11] G. Wilkinson,[59] M. Wilkinson,[63] I. Williams,[51] M. Williams,[60] M. R. J. Williams,[58] T. Williams,[49] F. F. Wilson,[53] M. Winn,[9] W. Wislicki,[33] M. Witek,[31] G. Wormser,[9] S. A. Wotton,[51] K. Wyllie,[44] D. Xiao,[68] Y. Xie,[68] A. Xu,[3] M. Xu,[68] Q. Xu,[4] Z. Xu,[6] Z. Xu,[3] Z. Yang,[3] Z. Yang,[62] Y. Yao,[63] L. E. Yeomans,[56] H. Yin,[68] J. Yu,[68,bb] X. Yuan,[63] O. Yushchenko,[40] K. A. Zarebski,[49] M. Zavertyaev,[13,w] D. Zhang,[68] L. Zhang,[3] W. C. Zhang,[3,cc] Y. Zhang,[44] A. Zhelezov,[14] Y. Zheng,[4] X. Zhu,[3] V. Zhukov,[11,36] J. B. Zonneveld,[54] and S. Zucchelli[17,h]

(LHCb Collaboration)

[1]*Centro Brasileiro de Pesquisas Físicas (CBPF), Rio de Janeiro, Brazil*
[2]*Universidade Federal do Rio de Janeiro (UFRJ), Rio de Janeiro, Brazil*
[3]*Center for High Energy Physics, Tsinghua University, Beijing, China*
[4]*University of Chinese Academy of Sciences, Beijing, China*
[5]*Institute Of High Energy Physics (ihep), Beijing, China*
[6]*Univ. Grenoble Alpes, Univ. Savoie Mont Blanc, CNRS, IN2P3-LAPP, Annecy, France*
[7]*Université Clermont Auvergne, CNRS/IN2P3, LPC, Clermont-Ferrand, France*
[8]*Aix Marseille Univ, CNRS/IN2P3, CPPM, Marseille, France*
[9]*LAL, Univ. Paris-Sud, CNRS/IN2P3, Université Paris-Saclay, Orsay, France*
[10]*LPNHE, Sorbonne Université, Paris Diderot Sorbonne Paris Cité, CNRS/IN2P3, Paris, France*
[11]*I. Physikalisches Institut, RWTH Aachen University, Aachen, Germany*
[12]*Fakultät Physik, Technische Universität Dortmund, Dortmund, Germany*
[13]*Max-Planck-Institut für Kernphysik (MPIK), Heidelberg, Germany*
[14]*Physikalisches Institut, Ruprecht-Karls-Universität Heidelberg, Heidelberg, Germany*
[15]*School of Physics, University College Dublin, Dublin, Ireland*
[16]*INFN Sezione di Bari, Bari, Italy*
[17]*INFN Sezione di Bologna, Bologna, Italy*
[18]*INFN Sezione di Ferrara, Ferrara, Italy*
[19]*INFN Sezione di Firenze, Firenze, Italy*
[20]*INFN Laboratori Nazionali di Frascati, Frascati, Italy*
[21]*INFN Sezione di Genova, Genova, Italy*
[22]*INFN Sezione di Milano-Bicocca, Milano, Italy*
[23]*INFN Sezione di Milano, Milano, Italy*
[24]*INFN Sezione di Cagliari, Monserrato, Italy*
[25]*INFN Sezione di Padova, Padova, Italy*
[26]*INFN Sezione di Pisa, Pisa, Italy*
[27]*INFN Sezione di Roma Tor Vergata, Roma, Italy*

[28]INFN Sezione di Roma La Sapienza, Roma, Italy
[29]Nikhef National Institute for Subatomic Physics, Amsterdam, Netherlands
[30]Nikhef National Institute for Subatomic Physics and VU University Amsterdam, Amsterdam, Netherlands
[31]Henryk Niewodniczanski Institute of Nuclear Physics Polish Academy of Sciences, Kraków, Poland
[32]AGH - University of Science and Technology, Faculty of Physics and Applied Computer Science, Kraków, Poland
[33]National Center for Nuclear Research (NCBJ), Warsaw, Poland
[34]Horia Hulubei National Institute of Physics and Nuclear Engineering, Bucharest-Magurele, Romania
[35]Institute of Theoretical and Experimental Physics NRC Kurchatov Institute (ITEP NRC KI), Moscow, Russia
[36]Institute of Nuclear Physics, Moscow State University (SINP MSU), Moscow, Russia
[37]Institute for Nuclear Research of the Russian Academy of Sciences (INR RAS), Moscow, Russia
[38]Yandex School of Data Analysis, Moscow, Russia
[39]Budker Institute of Nuclear Physics (SB RAS), Novosibirsk, Russia
[40]Institute for High Energy Physics NRC Kurchatov Institute (IHEP NRC KI), Protvino, Russia
[41]Petersburg Nuclear Physics Institute NRC Kurchatov Institute (PNPI NRC KI), Gatchina, Russia
[42]ICCUB, Universitat de Barcelona, Barcelona, Spain
[43]Instituto Galego de Física de Altas Enerxías (IGFAE), Universidade de Santiago de Compostela, Santiago de Compostela, Spain
[44]European Organization for Nuclear Research (CERN), Geneva, Switzerland
[45]Institute of Physics, Ecole Polytechnique Fédérale de Lausanne (EPFL), Lausanne, Switzerland
[46]Physik-Institut, Universität Zürich, Zürich, Switzerland
[47]NSC Kharkiv Institute of Physics and Technology (NSC KIPT), Kharkiv, Ukraine
[48]Institute for Nuclear Research of the National Academy of Sciences (KINR), Kyiv, Ukraine
[49]University of Birmingham, Birmingham, United Kingdom
[50]H.H. Wills Physics Laboratory, University of Bristol, Bristol, United Kingdom
[51]Cavendish Laboratory, University of Cambridge, Cambridge, United Kingdom
[52]Department of Physics, University of Warwick, Coventry, United Kingdom
[53]STFC Rutherford Appleton Laboratory, Didcot, United Kingdom
[54]School of Physics and Astronomy, University of Edinburgh, Edinburgh, United Kingdom
[55]School of Physics and Astronomy, University of Glasgow, Glasgow, United Kingdom
[56]Oliver Lodge Laboratory, University of Liverpool, Liverpool, United Kingdom
[57]Imperial College London, London, United Kingdom
[58]School of Physics and Astronomy, University of Manchester, Manchester, United Kingdom
[59]Department of Physics, University of Oxford, Oxford, United Kingdom
[60]Massachusetts Institute of Technology, Cambridge, Massachusetts, USA
[61]University of Cincinnati, Cincinnati, Ohio, USA
[62]University of Maryland, College Park, Maryland, USA
[63]Syracuse University, Syracuse, New York, USA
[64]Laboratory of Mathematical and Subatomic Physics, Constantine, Algeria
[associated with Universidade Federal do Rio de Janeiro (UFRJ), Rio de Janeiro, Brazil]
[65]Pontifícia Universidade Católica do Rio de Janeiro (PUC-Rio), Rio de Janeiro, Brazil
[associated with Universidade Federal do Rio de Janeiro (UFRJ), Rio de Janeiro, Brazil]
[66]South China Normal University, Guangzhou, China (associated with Center for High Energy Physics, Tsinghua University, Beijing, China)
[67]School of Physics and Technology, Wuhan University, Wuhan, China
(associated with Center for High Energy Physics, Tsinghua University, Beijing, China)
[68]Institute of Particle Physics, Central China Normal University, Wuhan, Hubei, China
(associated with Center for High Energy Physics, Tsinghua University, Beijing, China)
[69]Departamento de Fisica, Universidad Nacional de Colombia, Bogota, Colombia
(associated with LPNHE, Sorbonne Université, Paris Diderot Sorbonne Paris Cité, CNRS/IN2P3, Paris, France)
[70]Institut für Physik, Universität Rostock, Rostock, Germany (associated with Physikalisches Institut, Ruprecht-Karls-Universität Heidelberg, Heidelberg, Germany)
[71]Van Swinderen Institute, University of Groningen, Groningen, Netherlands
(associated with Nikhef National Institute for Subatomic Physics, Amsterdam, Netherlands)
[72]National Research Centre Kurchatov Institute, Moscow, Russia [associated with Institute of Theoretical and Experimental Physics NRC Kurchatov Institute (ITEP NRC KI), Moscow, Russia, Moscow, Russia]
[73]National University of Science and Technology "MISIS", Moscow, Russia [associated with Institute of Theoretical and Experimental Physics NRC Kurchatov Institute (ITEP NRC KI), Moscow, Russia, Moscow, Russia]
[74]National Research University Higher School of Economics, Moscow, Russia
(associated with Yandex School of Data Analysis, Moscow, Russia)
[75]National Research Tomsk Polytechnic University, Tomsk, Russia [associated with Institute of Theoretical and Experimental Physics NRC Kurchatov Institute (ITEP NRC KI), Moscow, Russia, Moscow, Russia]

[76]*Instituto de Fisica Corpuscular, Centro Mixto Universidad de Valencia - CSIC, Valencia, Spain (associated with ICCUB, Universitat de Barcelona, Barcelona, Spain)*
[77]*University of Michigan, Ann Arbor, Michigan, USA (associated with Syracuse University, Syracuse, New York, USA)*
[78]*Los Alamos National Laboratory (LANL), Los Alamos, New Mexico, USA (associated with Syracuse University, Syracuse, New York, USA)*

[a]Deceased.
[b]Also at Laboratoire Leprince-Ringuet, Palaiseau, France.
[c]Also at Università di Milano Bicocca, Milano, Italy.
[d]Also at Università di Modena e Reggio Emilia, Modena, Italy.
[e]Also at Novosibirsk State University, Novosibirsk, Russia.
[f]Also at Università di Ferrara, Ferrara, Italy.
[g]Also at LIFAELS, La Salle, Universitat Ramon Llull, Barcelona, Spain.
[h]Also at Università di Bologna, Bologna, Italy.
[i]Also at Università di Pisa, Pisa, Italy.
[j]Also at H.H. Wills Physics Laboratory, University of Bristol, Bristol, United Kingdom.
[k]Also at Università di Bari, Bari, Italy.
[l]Also at Sezione INFN di Trieste, Trieste, Italy.
[m]Also at Università di Genova, Genova, Italy.
[n]Also at Università degli Studi di Milano, Milano, Italy.
[o]Also at Universidade Federal do Triângulo Mineiro (UFTM), Uberaba-MG, Brazil.
[p]Also at AGH - University of Science and Technology, Faculty of Computer Science, Electronics and Telecommunications, Kraków, Poland.
[q]Also at Lanzhou University, Lanzhou, China.
[r]Also at Università di Padova, Padova, Italy.
[s]Also at Università di Cagliari, Cagliari, Italy.
[t]Also at MSU - Iligan Institute of Technology (MSU-IIT), Iligan, Philippines.
[u]Also at Scuola Normale Superiore, Pisa, Italy.
[v]Also at Hanoi University of Science, Hanoi, Vietnam.
[w]Also at P.N. Lebedev Physical Institute, Russian Academy of Science (LPI RAS), Moscow, Russia.
[x]Also at Università di Roma Tor Vergata, Roma, Italy.
[y]Also at Università di Roma La Sapienza, Roma, Italy.
[z]Also at Università della Basilicata, Potenza, Italy.
[aa]Also at Università di Urbino, Urbino, Italy.
[bb]Also at Physics and Micro Electronic College, Hunan University, Changsha City, China.
[cc]Also at School of Physics and Information Technology, Shaanxi Normal University (SNNU), Xi'an, China.